
Deep activity propagation via weight initialization in spiking neural networks

Aurora Micheli

Delft University of Technology
a.micheli@tudelft.nl

Olaf Booij

Delft University of Technology
o.booij@tudelft.nl

Jan van Gemert

Delft University of Technology
j.c.vangemert@tudelft.nl

Nergis Tömen

Delft University of Technology
n.tomen@tudelft.nl

Abstract

Spiking Neural Networks (SNNs) and neuromorphic computing offer bio-inspired advantages such as sparsity and ultra-low power consumption, providing a promising alternative to conventional networks. However, training deep SNNs from scratch remains a challenge, as SNNs process and transmit information by quantizing the real-valued membrane potentials into binary spikes. This can lead to information loss and vanishing spikes in deeper layers, impeding effective training. While weight initialization is known to be critical for training deep neural networks, what constitutes an effective initial state for a deep SNN is not well-understood. Existing weight initialization methods designed for conventional networks (ANNs) are often applied to SNNs without accounting for their distinct computational properties. In this work we derive an optimal weight initialization method specifically tailored for SNNs, taking into account the quantization operation. We show theoretically that, unlike standard approaches, this method enables the propagation of activity in deep SNNs without loss of spikes. We demonstrate this behavior in numerical simulations of SNNs with up to 100 layers across multiple time steps. We present an in-depth analysis of the numerical conditions, regarding layer width and neuron hyperparameters, which are necessary to accurately apply our theoretical findings. Furthermore, our experiments on MNIST demonstrate higher accuracy and faster convergence when using the proposed weight initialization scheme. Finally, we show that the newly introduced weight initialization is robust against variations in several network and neuron hyperparameters.

1 Introduction

Spiking Neural Networks (SNNs) are a class of artificial neural networks inspired by the dynamics of biological brains, where information is encoded and transmitted through discrete action potentials, or spikes [1, 20, 29]. This unique mode of communication enables SNNs to perform fast computations with remarkably low power consumption [21, 30], especially when combined with specialized neuromorphic hardware [5, 2, 40]. However, the task performance of SNNs is still not comparable with that of conventional artificial neural networks (ANNs). This discrepancy can be ascribed to the additional challenges associated with their training. Relying on the differentiability of the loss function with respect to the network parameters, ANNs are typically trained using a gradient descent algorithm. However, the discrete nature of spikes prevents the direct use of backpropagation in SNNs. Different methods such as ANN-SNN conversion [6, 7, 18] and backpropagation with surrogate functions [32, 43] have been proposed to circumvent this problem. Nevertheless, the proposed solutions haven't been sufficient to fully bridge the gap between SNNs and ANNs in terms of their

accuracy, without compromising the efficiency advantages of SNNs. Therefore, novel perspectives on other aspects of SNN optimization are evidently necessary.

Similarly to ANNs, in SNNs a suboptimal weight initialization can lead to vanishing or exploding gradients and hamper the training process [19, 37]. This issue becomes even more evident in deep networks [27]. The question of how to properly initialize the weights in a network has been widely explored in the ANN literature, and different initialization strategies have been proposed tailored to specific activation functions and weight distributions [12, 16, 31]. SNNs are currently initialized following standard schemes designed for ANNs, irrespective of their very distinct properties. Unlike ANNs, SNNs feature temporal dynamics, resetting mechanisms, information quantization and their activation function differs from those examined in the ANN literature. Hence, ANN initialization schemes are inadequate for SNNs and often lead to undesired effects such as vanishing or exploding spikes in deeper layers. In this paper:

- We analytically derive a weight initialization method which takes into account the specific activation function of a Spiking Neural Network, following the approach proposed in [16] for standard ANNs.
- We show that, unlike the standard method for the ReLU function, our initialization enables spiking activity to propagate from the input to the output layers of deep networks without being dissipated or amplified.
- We empirically validate our theoretical findings on simulations of deep SNNs up to 100 layers and 20 time steps and present an in-depth analysis on the impact of neuron and network hyperparameters on the results.
- We demonstrate on a simple classification task, how a proper initialization of the network weights can lead to better accuracy, faster convergence and lower latency.

2 Related work

A proper initialization method should avoid reducing or amplifying the magnitudes of input signals. In the context of ANNs, Glorot & Bengio in [12] address the issue of saturated units for the logistic sigmoid activation function and propose a new weight initialization scheme aimed at maintaining constant activations and gradient variance across layers. He et. al [16] extend this analysis to include the Rectified Linear Unit (ReLU) non-linearity and introduce what is conventionally called the Kaiming initialization, now widely adopted in deep ANNs.

To the best of our knowledge, there is little related work on initialisation schemes in SNNs. Some research regards ANN-SNN conversion as an initialization method for SNNs [36], thus necessarily depending on a traditional architecture as a starting point. In addition, conversion methods are limited to using a single, rate-based encoding strategy and do not allow for networks with arbitrary encoding schemes to be trained from scratch.

The problem of information propagation in SNNs has been indirectly addressed. In [35] and [45] the appropriate membrane leak factor and firing threshold are learnt during training. Similarly, in [41, 11] some learnable parameters are incorporated in the SNN to optimize the neuron firing rate. However, this approach inevitably results in increased computational complexity. A different way to control the magnitude of the output is to regularize the spike response. For instance, [24] introduces a global unsupervised firing rate normalization. Similarly, [44] and [23] adapt the concept of batch normalization [22] to SNNs and propose a batch normalization method along channel axes and time axes, respectively. Another possible way to regulate the information flow is by introducing additional terms in the loss function to constrain the distribution of membrane potentials [15, 14].

While the importance of effective weight initialization for training deep networks is largely acknowledged, the problem of determining what constitutes a good initial state for an SNN has been directly addressed in only a few studies. Some works attempt to empirically determine a suitable weight scale in the case of SNNs, but they often lack a solid theoretical foundation [27, 4, 42, 17]. In [8] the authors derive a new initialization strategy considering the asymptotic spiking response given a mean-driven input. However, this hinders the network from operating in an energy-efficient regime, characterized by very sparse spikes, and undermines the generalization to real-world data, which are usually noisy. [37] proposes a fluctuation-driven initialization scheme, but neglects both the spiking and the resetting mechanism. In [34] a specular approach similar to the one presented in

[16] is studied, yet the theoretical insights lack empirical validation or comparison with standard initialization methods for ANNs.

3 Methods

We first introduce the spiking neuron model in Section 3.1, then we derive a novel weight initialization method specifically designed for the activation function of a spiking neural network in Section 3.2.

3.1 The spiking neuron

The Leaky-Integrate-and-Fire (LIF) neuron [1] is one of the most popular models used in SNNs [20, 9] and neuromorphic hardware [2, 5] to emulate the functionality of biological neurons. The state of a LIF neuron at time t is given by the membrane potential $U(t)$ which evolves according to

$$\tau \frac{dU(t)}{dt} = -U(t) + RI(t), \quad (1)$$

where τ is the membrane time constant, R is the resistance of the membrane and $I(t)$ is the time-varying input current. Following previous works [23] we convert the continuous dynamic equation into a discrete equation using the Euler method with discretization time step Δt . We can represent the membrane potential u at time step t as:

$$u^t = \beta u^{t-1} + \sum_j w_j x_j^t, \quad (2)$$

where $\beta \propto (1 - \Delta t/\tau)$ is a leak factor $\in [0, 1]$ governing the rate at which the membrane potential decays over time, j is the index of the pre-synaptic neuron, w_j represents the weight of the connection between the pre- and post-synaptic neurons and x_j is the binary spike activation. When the membrane potential u exceeds a firing threshold θ , the neuron emits a binary output spike $x = 1$. After firing, the membrane potential is reset by subtracting from its value the threshold θ . This operation is conventionally called a soft reset, and it differs from a hard reset (resetting u to 0 after a spike) because it minimizes the loss of information, therefore achieving better performance [13].

3.2 Weight initialization for a spiking neural network

Our derivation is inspired by He et al. [16], which suggests that an effective weight initialization should enable information flow across many network layers by keeping the variance of the input to each layer constant. In our analysis, we examine the variance of responses within each layer of a fully-connected SNN initialized at time step $t = 0$. For a generic layer l with m neurons:

$$\mathbf{u}_l = \mathbf{w}_l \mathbf{x}_l \quad (3)$$

$$\mathbf{x}_l = f(\mathbf{u}_{l-1}) \quad (4)$$

Here $\mathbf{x}_l \in \{0, 1\}^n$ is a binary vector representing the n input spikes, $\mathbf{w}_l \in \mathbb{R}^{m \times n}$ is the weight matrix and $\mathbf{u}_l \in \mathbb{R}^m$ represents the membrane potentials of neurons in layer l . \mathbf{x}_l is obtained by applying the activation function f to the membrane potentials of layer $l - 1$. In a conventional SNN f is defined as the Heaviside step function:

$$f(\mathbf{u}_{l-1}) = \begin{cases} 1, & \text{if } u_{l-1} > \theta \\ 0, & \text{if } u_{l-1} < \theta \end{cases} \quad (5)$$

where u_{l-1} are the elements of \mathbf{u}_{l-1} and $\theta > 0$ is the neurons firing threshold. We assume that the elements of \mathbf{w}_l are mutually independent and share the same distribution (i.i.d.). Following [16] and [12], the elements of \mathbf{x}_l are also considered to be mutually independent and identically distributed (i.i.d.). Lastly, \mathbf{w}_l and \mathbf{x}_l are independent of each other. We can then write:

$$\text{Var}[u_l] = n_l \text{Var}[w_l x_l]. \quad (6)$$

Here u_l , w_l , and x_l represent each random variable element in \mathbf{u}_l , \mathbf{w}_l and \mathbf{x}_l respectively. We choose w_l to be symmetrically distributed around 0. Since w_l and x_l are independent of each other, we can rewrite the variance of their product as:

$$\text{Var}[u_l] = n_l \text{Var}[w_l] E[x_l^2], \quad (7)$$

where $E[x_l^2]$ is the expected value of x_l^2 . It is worth noting that the expression $E[x_l^2]$ strongly depends on the network activation function. Here is where our derivations crucially differ from He et al. [16].

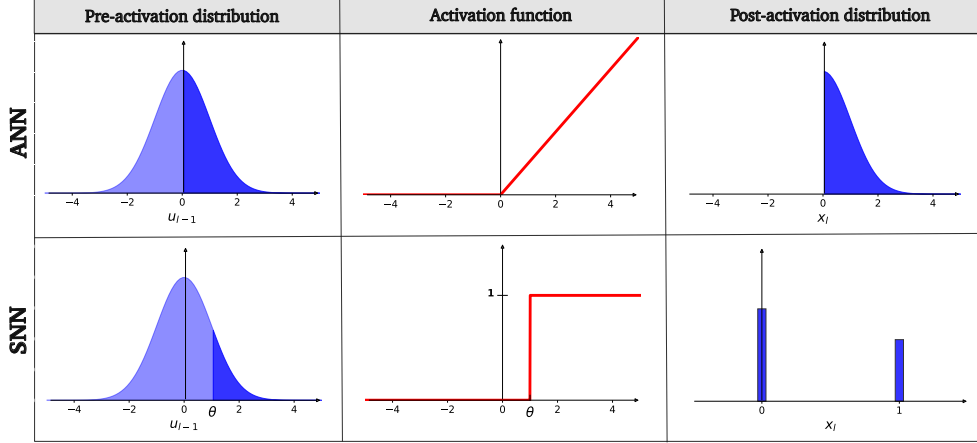


Figure 1: Comparison of standard activation functions for ANNs (*top*) and SNNs (*bottom*). When applied to pre-activation distribution u_{l-1} (*left*) the SNN thresholding mechanism (*middle*) generates binarized activations x_l (*right*). The dark shaded areas of u_{l-1} correspond to the fraction of neurons which will be activated and provide non-zero input to the next layer. With identical input distributions, this fraction is considerably lower for SNNs. This highlights why weight initializations optimized for ReLU will lead to vanishing activity in deep SNNs.

By assuming that u_{l-1} is zero-centered and symmetric around its mean, for a ReLU activation function, $x_l = \max(0, u_{l-1})$, one obtains $E[x_l^2] = \frac{1}{2}\text{Var}[u_{l-1}]$. This result stems from the fact that the ReLU function preserves exactly the positive half of the distribution it acts upon. As depicted in Figure 1, this doesn't hold true for the activation function of SNNs where, by definition, $\theta > 0$. This difference leads to considerably sparser activations in SNNs and to a different conclusion about optimal weight initializations from [16]. In the case of an SNN, we can express $E[x_l^2]$ as:

$$E[x_l^2] = \sum_{j=1}^n x_l^j{}^2 P(x_l = x_l^j). \quad (8)$$

Again, the binary elements $x_l^j \in \{0, 1\}$ represent spikes. Applying the SNN activation function (5) to Eq. 8, we find that $E[x_l^2] = P(u_{l-1} > \theta)$. Equation 7 can then be rewritten as:

$$\text{Var}[u_l] = n_l \text{Var}[w_l] P(u_{l-1} > \theta). \quad (9)$$

As commonly done in recent works [14, 35, 10, 11], we consider a real-valued input I_0 encoded to binary spikes using the first layer of the SNN. When feeding the input to the membrane potentials u_0 of the initial layer, then $u_0 = I_0$ and u_0 trivially follows the same distribution as the input. We let I_0 be standard normal distributed $I_0 \sim \mathcal{N}(\mu = 0, \sigma^2 = 1)$, thus $\text{Var}[u_0] = 1$, $E[u_0] = 0$. A proper initialization method should avoid reducing or amplifying the magnitudes of the input signals when propagated across the network layers. In other words, the objective is to prevent vanishing or exploding spikes. This condition can be met if $\text{Var}[u_l] = 1$ for every layer l , which lets us simplify Eq. 9 and leads to a zero-mean Gaussian weight distribution with variance:

$$\text{Var}[w_l] = \frac{1}{n_l P(u_{l-1} > \theta)} \quad (10)$$

Equation 10 is our proposed weight initialization method for training deep SNNs. Note that in terms of architecture parameters, it only depends on the number of input neurons n .

Because u_{l-1} is symmetric around 0 and $\theta > 0$, then $P(u_{l-1} > \theta) < \frac{1}{2}$. It is therefore important to note that:

$$\frac{1}{n_l P(u_{l-1} > \theta)} > \frac{2}{n_l}, \quad (11)$$

Where $\frac{2}{n_l}$ is the standard initialization for a ReLU network [16]. Thus, initializing the weights of an SNN using a method designed for conventional ANNs with ReLU activation functions does not ensure the propagation of information from the input throughout the network.

4 Empirical validation

In this section, we empirically validate our theoretical findings using numerical simulations of deep SNNs. In 4.1, we show that the simulations agree with our theoretical derivation and demonstrate that our weight initialization is able to effectively propagate activity throughout a deep SNN. Conversely, the initialization method tailored for the ReLU activation function does not achieve similar results: often it leads to vanishing spikes. We also discuss how parameters like firing threshold and layer width affect our theoretical findings, and we highlight the presence of finite-size effects in SNNs. In 4.2 we expand our analysis to include multi-time-step simulations. We show that our new initialization strategy maintains its ability to conserve the level of activity across layers and time steps, and we explore variations in neuron hyperparameters which uphold this property.

4.1 Validation with numerical simulations

For the following analysis, unless otherwise specified, we consider fully-connected SNNs with 100 layers and $n = 1000$ LIF neurons in each layer. The input I_0 is real-valued and randomly drawn from $\mathcal{N}(\mu = 0, \sigma^2 = 1)$. Consistently with the derivation in 3.2, we encode the inputs to binary spikes by feeding them to the membrane potentials of the initial LIF layer u_0 .

We investigate the behavior of activity propagation under different weight initialization schemes and compare our method against the prevailing choice for conventional ANNs: Kaiming initialization ([16]). The weights in the network are therefore randomly initialized respectively from $\mathcal{N}(0, \sqrt{\frac{1}{nP(u_0 > \theta)}})$ (our method) and $\mathcal{N}(0, \sqrt{\frac{2}{n}})$ (Kaiming), where n is the layer width. Since $u_0 \sim \mathcal{N}(0, 1)$, $P(u_0 > \theta)$ is defined as:

$$P(u_0 > \theta) = \int_{\theta}^{\infty} \frac{1}{\sqrt{2\pi}} e^{-\frac{u_0^2}{2}} du_0. \quad (12)$$

The integral in Eq. 12 doesn't have a closed-form solution, but it can be numerically estimated using the error function [3]. We recall from 3.2 that, to retain the activity over depth, we aim to conserve $\text{Var}[u_l]$ across the layers. To investigate the change in this variance across depth, we initialize the network at time $t = 0$, propagate the input across its layers, record the values of the membrane potentials u_l in every layer l and compute their variance. Figure 2 shows how $\text{Var}[u_l]$ evolves with depth for the 2 different initialization schemes and for 6 different values of the firing threshold θ . For every different value of θ , we run the simulation 20 times and plot the average. The shaded areas represent the standard deviation over the different runs.

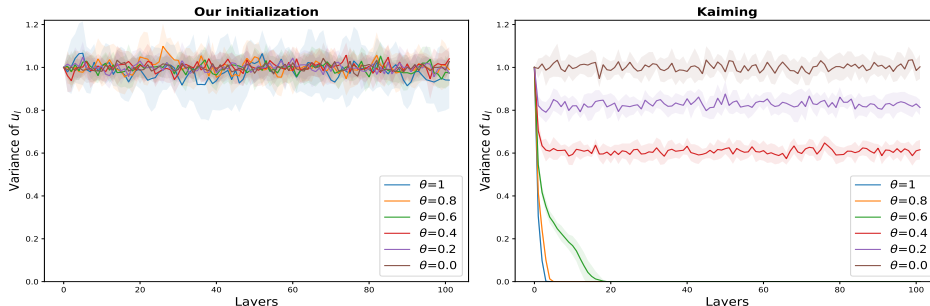


Figure 2: Propagation of $\text{Var}[u_l]$ across network layers for (left) our initialization scheme and (right) Kaiming for six firing threshold values (θ). For all θ , our proposed initialization method enables information propagation across all 100 layers. In contrast, Kaiming initialization leads to information dissipation across layers, particularly evident with higher threshold values. Each simulation was repeated 20 times, and the shaded areas represent the standard deviation over these runs.

The results (Figure 2, left) demonstrate that in an SNN initialized with our proposed method, the variance $\text{Var}[u_i]$ of the neuron states stays constant across layers as the theory predicts. Specifically, we show that neuronal activity seamlessly propagates across all 100 layers, regardless of the threshold value θ . Conversely, when the network weights are initialized using Kaiming, information dissipates across the layers, with this effect becoming more pronounced as firing threshold values increase. Notably, using Kaiming, the only viable method to effectively preserve information is by setting $\theta = 0$, where the activation function becomes effectively equivalent to ReLU and the network is reduced to an ANN.

We then explore the scalability of our approach with respect to the width of the layers. First, we note that, the higher the firing threshold, the smaller the area defined by the integral in Eq. 12. This means that the probability of spiking is decreased. For high θ , where spiking probability is theoretically low, as we reduce the number of neurons n in each layer, it becomes increasingly less likely to numerically sample the estimated ‘average’ number of spikes in the simulations. Specifically, since we cannot sample the necessary number of spikes in layers with small n , the activity will die out in deeper layers. This deviation of simulations from theory does not happen if the layer size n is large enough compared to the spiking probability of Eq. 12. We refer to this phenomenon as a finite-size effect, and its impact on the propagation of information in the network is illustrated in Figure 3.

The results demonstrate that a 100-layer network with layer width $n = 100$ struggles to retain the spiking activity in deeper layers as we increase θ (Figure 3, left). The finite-size effect becomes particularly prominent for values of θ exceeding 0.85. However, when we increase the layer width from 100 to 600, we observe a significant reduction in the prominence of this effect, except for the case of $\theta = 1$. We find this insight particularly relevant in the context of designing SNN architectures and determining their hyperparameters. Due to the thresholding operation serving as the activation function in an SNN and the binarization of activations, the combination of the number of neurons and firing threshold significantly influences the network’s behavior. Specific configurations of these parameters can in fact complicate information propagation if proper adjustments are not implemented.

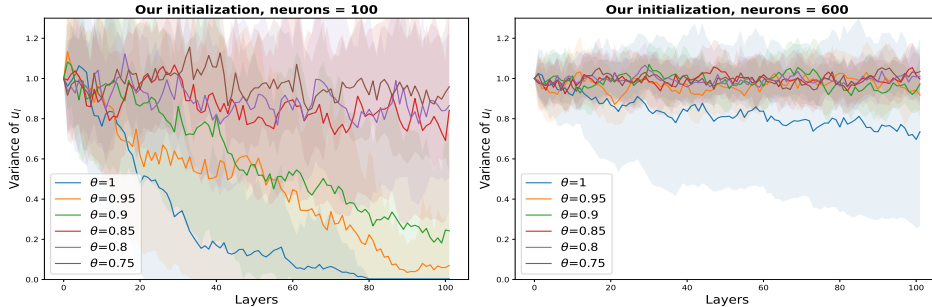


Figure 3: Impact of the finite-size effect on the propagation of $\text{Var}[u_i]$ across layers. As the number of neurons decreases and spiking threshold θ increases, the discrepancy between empirical and theoretical results becomes more pronounced. (Left): $n = 100$. The network can’t conserve activity over depth for $\theta > 0.85$. (Right): $n = 600$. By increasing the number of neurons the finite-size effect becomes less pronounced even for higher values of θ . Each simulation was repeated 20 times, and the shaded areas represent the standard deviation over these runs.

4.2 Extension to multiple time steps

SNNs demonstrate their main advantages when processing time-dependent input. This is because spiking neurons, inspired by biological counterparts, possess an intrinsic memory, the membrane potential u , which naturally integrates information over time. Through precise spike timing, SNNs can process temporal information with greater computational power than ANNs [29]. This makes them well-suited for tasks involving dynamic temporal patterns, such as speech recognition and video analysis [33, 39, 28].

In this section we extend the analysis of Section 4.1 to activity propagation in space *and* time. We address the question of how weight initialization affects information propagation in multiple time-step simulations of deep SNNs. As in Section 4.1, we employ fully-connected SNNs of 100 layers with $n = 1000$ neurons in each layer. We consider LIF neurons with soft reset and numerically compute

the discrete-time dynamics based on Eq. 2. The dynamics of the membrane potentials including the reset term is given by:

$$u_l^t = w_l^t x_l^t + \beta u_l^{t-1} - x_{l+1}^{t-1} \theta \quad (13)$$

for time step $t > 0$ and layer l . $\beta \in [0, 1]$ is again the leak factor. For comparison, network weights are randomly initialized either using our initialization scheme or Kaiming, and the inputs are randomly drawn from $\sim \mathcal{N}(0, 1)$, same as in Section 4.1. Differently, in this section, we iteratively feed the input (constant over time) to the membrane potentials of the initial LIF layer u_0^t at every time step t . We compute the variance of the membrane potentials u_l^t and the total number of spikes at every layer l and time step t , for a total of $T = 20$ time steps. We repeat each simulation 10 times, and report their average.

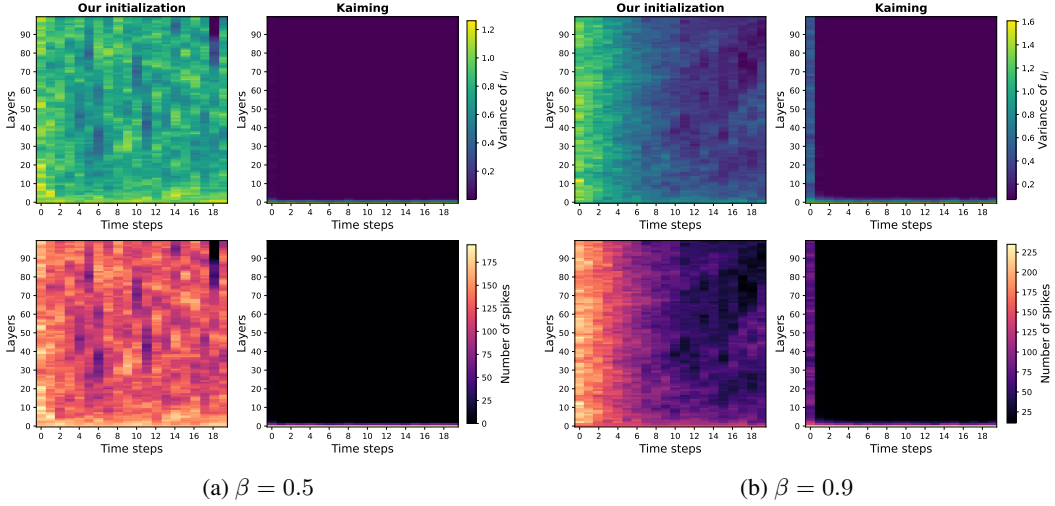


Figure 4: Propagation of $\text{Var}[u_l^t]$ (*top row*) and number of spikes (*bottom row*) across layers and time steps for our initialization method and Kaiming averaged over 10 runs. **(a)** Our proposed weight initialization preserves activity and propagates spikes through 100 layers and 20 time steps. In contrast, with Kaiming initialization neuronal activity rapidly dies out. **(b)** The effect of the leak and reset terms becomes more pronounced for high values of β and pushes the network into the dissipative regime. However, with our proposed initialization method, we can still successfully retrieve an output.

The network initialized with our method succeeds in conserving the $\text{Var}[u_l^t]$ across both space and time, whereas the network initialized with Kaiming fails (Fig. 4a). Conserving $\text{Var}[u_l^t]$ is crucial, as it means conserving the number of spikes, and therefore ensuring a consistent network output. An improper weight initialization can in fact swiftly lead to vanishing spikes and cause the network activity to completely die out.

Although our mathematical derivation does not explicitly take time into account, unlike methods derived for ANNs, it considers the specific SNN activation function, and by keeping the variance of the membrane potentials u_l constant, it aims to indirectly keep the variance of the layer input $w_l x_l$ constant (Eq. 3). This helps to effectively propagate information also across multiple time steps. Nevertheless, we expect deviations from theory, caused by the leak and reset terms (Eq. 13). In particular, the reset operation has a non-negligible effect on the distribution of the membrane potentials. This operation violates the assumption that u_l^t is always normally distributed and symmetrically centered around 0 (see Appendix 7). However, how well the normal distribution still holds as an approximation depends on neuron hyperparameters. For example, deviations from theory are visible at higher values of β . A larger β leads to broader distributions of u_l^t , and thus to a more abrupt change in the distributions when neurons with $u_l^t > \theta$ are reset. As illustrated in Fig. 4b, when $\beta = 0.9$, the network dissipates energy over time. We attribute this dissipation to the shift in u_l^t distributions. Still, we note that with our proposed initialization method, we can still successfully retrieve an output, unlike with Kaiming.

5 Experiments on MNIST

In this section, we evaluate how our variance-conserving weight initialization for SNNs can translate into accelerated training, improved accuracy and lower latency. To that end, we conduct object classification experiments using the MNIST digits dataset [26]. The dataset is composed of 50,000 training samples and 10,000 test samples, where each sample is a 28×28 pixel grey-scale image of one of the 10 digits. The images are normalized to have mean 0 and variance 1, in line with the assumptions used in the derivations. As in Section 4 the inputs are encoded to binary spikes using the first LIF layer. The final layer of the network outputs binary spikes, which are accumulated over time steps and passed to the cross-entropy loss function. Unless otherwise specified, we employ a fully-connected SNN consisting of 10 layers, each comprising $n = 600$ LIF neurons with soft reset. We set $\theta = 1$ and $\beta = 0.5$.

Commonly, SNNs performing spike-count based object classification use a large number of total time steps T , in order to accumulate a reliable number of spikes at the output layer. A typical range of T can be between 10 and a few thousand [38]. Here, in order to demonstrate the power of a good weight initialization, we set the number of total time steps to $T = 3$. We hypothesize that initializations which enable constant information propagation across depth might also enable inference with low latency, where there is no need to wait for many time steps to accumulate the necessary number of output spikes.

The network is trained for 150 epochs using backpropagation through time (BPTT) [27] and the arctan surrogate gradient function [11]. We utilize the Adam optimizer [25] with a learning rate of 1×10^{-3} and employ cosine annealing scheduling. The runtime for each experiment is approximately 2 hours on a single GPU. Our weight initialization method is compared to Kaiming, as in previous sections.

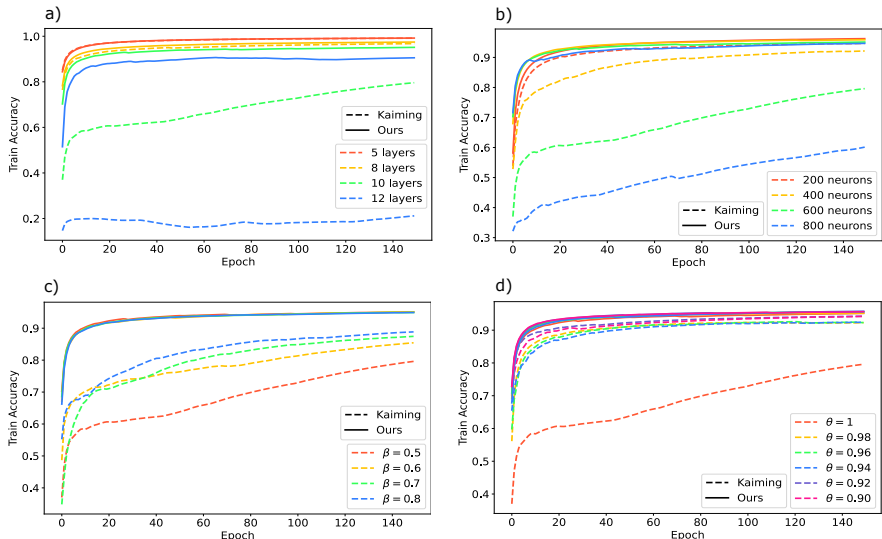


Figure 5: Training accuracy on MNIST for different values of **a)** network depth, **b)** layer width, **c)** β and **d)** θ . We compare our proposed initialization method (solid lines) to Kaiming (dashed lines) and find that it achieves better training accuracy and faster convergence.

The results illustrated in Figure 5 and Figure 6 show that our method generally allows an SNN to converge faster during training and to achieve better training and test accuracy than Kaiming for different values of network and neuron parameters. More specifically, we repeat the experiments for different values of network depth, layer width, β and θ and observe that our method is robust to these variations. We observe that networks initialized with Kaiming tend to struggle with convergence and demonstrate lower task performance. Consistent with both theoretical insights and empirical findings presented in previous sections, we attribute this behavior to inadequate activity propagation. Specifically, we note that training becomes increasingly challenging with deeper networks, higher values of θ (resulting in fewer neurons emitting spikes) and lower values of β (leading to less information retention from the previous time step). Nevertheless, our proposed initialization is robust

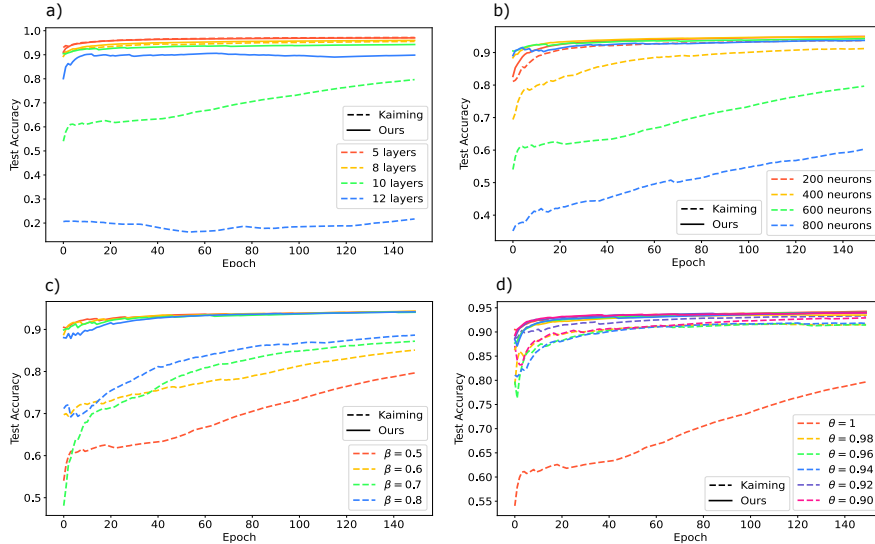


Figure 6: Test accuracy on MNIST for different values of **a)** network depth, **b)** layer width, **c)** β and **d)** θ . Similar to the training accuracy (Fig. 5) we find that our proposed initialization (solid lines) achieves better generalization than Kaiming (dashed lines).

against changes in these critical hyperparameters when compared to the commonly used Kaiming initialization scheme.

6 Conclusion and Discussion

In recent years, the introduction of new initialization techniques has significantly contributed to the success of ANNs, particularly in enabling the training of deeper architectures. It’s evident that proper weight initialization plays a crucial role in achieving optimal accuracy and facilitating fast convergence. In this paper, we address the problem of weight initialization in Spiking Neural Networks (SNNs) and show how the techniques developed for ANNs, such as Kaiming initialization, are inadequate for SNNs. Unlike standard non-linearities for ANNs, the thresholding mechanism in SNNs produces binarized activations. Consequently, combining SNNs with weight initializations optimized for ReLU results in the well-known vanishing spikes problem. This inevitably leads to information loss in deeper layers. Here, we analytically derive a novel weight initialization method which takes into account the specific activation function of SNNs. We empirically demonstrate that, in contrast to Kaiming, our initialization enables spiking activity to propagate from the input to the output layers of deep networks without being dissipated or amplified, a necessary condition for effective network training. Similar to the popular Kaiming initialization for ANNs, our weight initialization depends only on the number of input neurons n to a layer. Therefore, our approach is broadly applicable to all deep, spiking network architectures with fixed connectivity maps. In addition, we demonstrate that our proposed initialization is robust against variations in several important network and neuron hyperparameters, which can enable deep activity propagation for diverse models and machine learning tasks. To further improve training in deep SNNs, we highlight that, due to the specific properties of the SNN activation function, the width of the network and the firing threshold might significantly affect information propagation.

A limitation of our approach is that the proposed initialization does not account for the temporal dynamics of the neuron membrane potentials u_i , specifically the effects of the leakage and the resetting operation. Specifically, after neurons which emit a spike are reset, our assumption that u_i is normally distributed around zero is violated. We observe that the extent to which the normal distribution remains a valid approximation depends on the neuron hyperparameters. Our initialization strategy, unlike Kaiming, still helps to effectively propagate information, also across multiple time steps. However, the theory can be expanded to explicitly take into account the temporal variations in u_i . Another assumption of our derivation is that the activations x_i are mutually independent. However, this assumption is typically violated in the case of real-world data, such as images. Empirically, in

section 5 we illustrate how, for an SNN trained on MNIST, our variance-conserving initialization scheme still translates into accelerated training, improved accuracy and low latency compared to Kaiming. Nevertheless, we acknowledge the necessity of extending this analysis to more complex architectures and datasets, in order to evaluate its effectiveness in various settings.

References

- [1] L F Abbott. Lapicque’s introduction of the integrate-and-fire model neuron (1907). Technical Report 6, 1999.
- [2] Filipp Akopyan, Jun Sawada, Andrew Cassidy, Rodrigo Alvarez-Icaza, John Arthur, Paul Merolla, Nabil Imam, Yutaka Nakamura, Pallab Datta, Gi Joon Nam, Brian Taba, Michael Beakes, Bernard Brezzo, Jente B. Kuang, Rajit Manohar, William P. Risk, Bryan Jackson, and Dharmendra S. Modha. TrueNorth: Design and Tool Flow of a 65 mW 1 Million Neuron Programmable Neurosynaptic Chip. *IEEE Transactions on Computer-Aided Design of Integrated Circuits and Systems*, 34(10):1537–1557, 10 2015.
- [3] L.C. Andrews. *Special Functions of Mathematics for Engineers*. SPIE Optical Engineering Press, 1998.
- [4] Guillaume Bellec, Darjan Salaj, Anand Subramoney, Robert Legenstein, and Wolfgang Maass. Long short-term memory and learning-to-learn in networks of spiking neurons. 3 2018.
- [5] Mike Davies, Narayan Srinivasa, Tsung Han Lin, Gautham Chinya, Yongqiang Cao, Sri Harsha Choday, Georgios Dimou, Prasad Joshi, Nabil Imam, Shweta Jain, Yuyun Liao, Chit Kwan Lin, Andrew Lines, Ruokun Liu, Deepak Mathaikutty, Steven McCoy, Arnab Paul, Jonathan Tse, Guruguhathan Venkataramanan, Yi Hsin Weng, Andreas Wild, Yoonseok Yang, and Hong Wang. Loihi: A Neuromorphic Manycore Processor with On-Chip Learning. *IEEE Micro*, 38(1):82–99, 1 2018.
- [6] Shikuang Deng and Shi Gu. Optimal Conversion of Conventional Artificial Neural Networks to Spiking Neural Networks. 2 2021.
- [7] Jianhao Ding, Zhaofei Yu, Yonghong Tian, and Tiejun Huang. Optimal ANN-SNN Conversion for Fast and Accurate Inference in Deep Spiking Neural Networks. 5 2021.
- [8] Jianhao Ding, Jiyuan Zhang, Zhaofei Yu, and Huang Tiejun. Accelerating Training of Deep Spiking Neural Networks with Parameter Initialization. 2022.
- [9] Jason K. Eshraghian, Max Ward, Emre Neftci, Xinxin Wang, Gregor Lenz, Girish Dwivedi, Mohammed Bennamoun, Doo Seok Jeong, and Wei D. Lu. Training Spiking Neural Networks Using Lessons From Deep Learning. 9 2021.
- [10] Wei Fang, Zhaofei Yu, Yanqi Chen, Tiejun Huang, Timothée Masquelier, and Yonghong Tian. Deep Residual Learning in Spiking Neural Networks. 2 2021.
- [11] Wei Fang, Zhaofei Yu, Yanqi Chen, Timothée Masquelier, Tiejun Huang, and Yonghong Tian. Incorporating Learnable Membrane Time Constant to Enhance Learning of Spiking Neural Networks. In *Proceedings of the IEEE International Conference on Computer Vision*, pages 2641–2651. Institute of Electrical and Electronics Engineers Inc., 2021.
- [12] Xavier Glorot and Yoshua Bengio. Understanding the difficulty of training deep feedforward neural networks. Technical report.
- [13] Yufei Guo, Yuanpei Chen, Liwen Zhang, Yinglei Wang, Xiaode Liu, Xinyi Tong, Yuanyuan Ou, Xuhui Huang, and Zhe Ma. Reducing Information Loss for Spiking Neural Networks. Technical report.
- [14] Yufei Guo, Xiaode Liu, Yuanpei Chen, Liwen Zhang, Weihang Peng, Yuhan Zhang, Xuhui Huang, and Zhe Ma. RMP-Loss: Regularizing Membrane Potential Distribution for Spiking Neural Networks. 8 2023.
- [15] Yufei Guo, Xinyi Tong, Yuanpei Chen, Liwen Zhang, Xiaode Liu, Zhe Ma, and Xuhui Huang. RecDis-SNN: Rectifying Membrane Potential Distribution for Directly Training Spiking Neural Networks. Technical report.
- [16] Kaiming He, Xiangyu Zhang, Shaoqing Ren, and Jian Sun. Delving Deep into Rectifiers: Surpassing Human-Level Performance on ImageNet Classification. 2 2015.

- [17] Luca Herranz-Celotti and Jean Rouat. Stabilizing Spiking Neuron Training. 2 2022.
- [18] Nguyen-Dong Ho and Ik-Joon Chang. TCL: an ANN-to-SNN Conversion with Trainable Clipping Layers. 8 2020.
- [19] Sepp Hochreiter and Jürgen Schmidhuber. Long Short-Term Memory. *Neural Computation*, 9(8):1735–1780, 11 1997.
- [20] Eric Hunsberger and Chris Eliasmith. Spiking Deep Networks with LIF Neurons. 10 2015.
- [21] Giacomo Indiveri, Bernabé Linares-Barranco, Tara Julia Hamilton, André van Schaik, Ralph Etienne-Cummings, Tobi Delbruck, Shih Chii Liu, Piotr Dudek, Philipp Häfliger, Sylvie Renaud, Johannes Schemmel, Gert Cauwenberghs, John Arthur, Kai Hynna, Fopefolu Folowosele, Sylvain Saighi, Teresa Serrano-Gotarredona, Jayawan Wijekoon, Yingxue Wang, and Kwabena Boahen. Neuromorphic silicon neuron circuits, 2011.
- [22] Sergey Ioffe and Christian Szegedy. Batch Normalization: Accelerating Deep Network Training by Reducing Internal Covariate Shift. 2 2015.
- [23] Youngeun Kim and Priyadarshini Panda. Revisiting Batch Normalization for Training Low-latency Deep Spiking Neural Networks from Scratch. 10 2020.
- [24] Youngeun Kim and Priyadarshini Panda. Optimizing Deeper Spiking Neural Networks for Dynamic Vision Sensing. *Neural Networks*, 144:686–698, 12 2021.
- [25] Diederik P. Kingma and Jimmy Ba. Adam: A Method for Stochastic Optimization. 12 2014.
- [26] Y. Lecun, L. Bottou, Y. Bengio, and P. Haffner. Gradient-based learning applied to document recognition. *Proceedings of the IEEE*, 86(11):2278–2324, 1998.
- [27] Jun Haeng Lee, Tobi Delbruck, and Michael Pfeiffer. Training Deep Spiking Neural Networks using Backpropagation. 8 2016.
- [28] Qianhui Liu, Dong Xing, Huajin Tang, De Ma, and Gang Pan. Event-based Action Recognition Using Motion Information and Spiking Neural Networks. Technical report, 2021.
- [29] Wolfgang Maass. Networks of Spiking Neurons: The Third Generation of Neural Network Models. Technical Report 9, 1997.
- [30] Wolfgang Maass and Henry Markram. On the computational power of circuits of spiking neurons. *Journal of Computer and System Sciences*, 69(4):593–616, 2004.
- [31] Dmytro Mishkin and Jiri Matas. All you need is a good init. 11 2015.
- [32] Emre O. Neftci, Hesham Mostafa, and Friedemann Zenke. Surrogate Gradient Learning in Spiking Neural Networks: Bringing the Power of Gradient-based optimization to spiking neural networks. *IEEE Signal Processing Magazine*, 36(6):51–63, 11 2019.
- [33] Thomas Pellegrini, Romain Zimmer, and Timothée Masquelier. Low-activity supervised convolutional spiking neural networks applied to speech commands recognition. 11 2020.
- [34] Nicolas Perez-Nieves and Dan F. M Goodman. Spiking Network Initialisation and Firing Rate Collapse. 5 2023.
- [35] Nitin Rathi and Kaushik Roy. DIET-SNN: Direct Input Encoding With Leakage and Threshold Optimization in Deep Spiking Neural Networks. 8 2020.
- [36] Nitin Rathi, Gopalakrishnan Srinivasan, Priyadarshini Panda, and Kaushik Roy. Enabling Deep Spiking Neural Networks with Hybrid Conversion and Spike Timing Dependent Backpropagation. 5 2020.
- [37] Julian Rossbroich, Julia Gygax, and Friedemann Zenke. Fluctuation-driven initialization for spiking neural network training. 6 2022.
- [38] Kaushik Roy, Akhilesh Jaiswal, and Priyadarshini Panda. Towards spike-based machine intelligence with neuromorphic computing. *Nature*, 575(7784):607–617, 11 2019.
- [39] Jibin Wu, Emre Yilmaz, Malu Zhang, Haizhou Li, and Kay Chen Tan. Deep Spiking Neural Networks for Large Vocabulary Automatic Speech Recognition. *Frontiers in Neuroscience*, 14, 3 2020.
- [40] Kashu Yamazaki, Viet Khoa Vo-Ho, Darshan Bulsara, and Ngan Le. Spiking Neural Networks and Their Applications: A Review, 7 2022.

- [41] Bojian Yin, Federico Corradi, and Sander M. Bohté. Effective and Efficient Computation with Multiple-timescale Spiking Recurrent Neural Networks. 5 2020.
- [42] Friedemann Zenke and Tim P Vogels. The remarkable robustness of surrogate gradient learning for instilling complex function in spiking neural networks.
- [43] Friedemann Zenke and Tim P. Vogels. The Remarkable Robustness of Surrogate Gradient Learning for Instilling Complex Function in Spiking Neural Networks. *Neural computation*, 33(4):899–925, 3 2021.
- [44] Hanle Zheng, Yujie Wu, Lei Deng, Yifan Hu, and Guoqi Li. Going Deeper With Directly-Trained Larger Spiking Neural Networks. Technical report, 2021.
- [45] Romain Zimmer, Thomas Pellegrini, Srisht Fateh Singh, and Timothée Masquelier. Technical report: supervised training of convolutional spiking neural networks with PyTorch. 11 2019.

7 Appendix

The reset operation violates the assumption that u_i^t is always normally distributed and symmetrically centered around 0, especially for higher values of β . In Figure 7 we show the values of skewness and excess kurtosis for u_i^t across layers and time steps in the case of $\beta = 0.9$. Skewness measures the degree of asymmetry of the distribution, while excess kurtosis measures the degree of peakedness and flatness of a distribution. A normal distribution has 0 skewness and 0 excess kurtosis. We note how u_i^t tends to a left-skewed and heavy-tailed distribution.

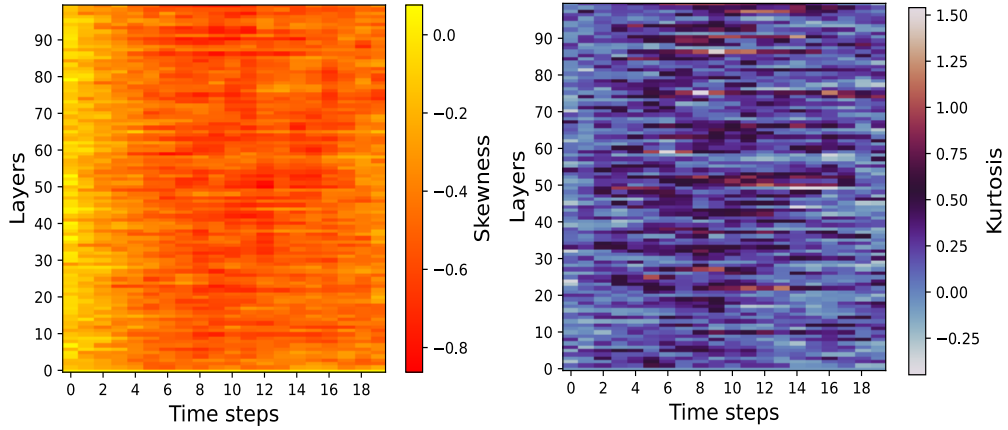


Figure 7: Skewness (*left*) and excess kurtosis (*right*) of u_i^t across layers and time steps for $\beta = 0.9$.